

Syntheses, Structural Characterizations, and Catalytic Behavior of *ansa*-Metallocene Complexes Derived from 1,1-Dicyclopentadienyl-1-silacycloalkanes

Sung-Joon Kim,[†] Young-Joo Lee,[†] Eugene Kang,[†] Sang Hern Kim,^{*,‡} Jaejung Ko,^{*,†} Byunyeol Lee,[§] Minserk Cheong,[‡] Il-Hwan Suh,[†] and Sang Ook Kang^{*,†}

Department of Chemistry, Korea University, 208 Seochang, Chochiwon, Chung-nam 339-700, Korea, Department of Chemical Technology, Hanbat National University, Daejeon 305-719, Korea, Department of Molecular Science, Ajou University, Suwon 130-743, Korea, and Department of Chemistry and Research Institute for Basic Sciences, Kyung Hee University, Seoul 130-701, Korea

Received April 22, 2003

1,1-Dicyclopentadienyl-1-silacycloalkanes (**2**) were prepared by condensation of cyclopentadiene with appropriate 1,1-dichloro-1-silacycloalkanes [(cyclo)SiCl₂ (**1**); cyclo = C_nH_{2n}, n = 3, 4, 5]. Dilithium salts of **2** were subsequently transformed into the corresponding *ansa*-metallocene complexes [{η⁵-Cp₂-(cyclo)Si}MCl₂] (M = Ti (**3**), Zr (**4**), Hf (**5**)). The molecular structures of **3b**, **3c**, **4b**, and **4c** were determined by X-ray crystallography. As a result of the formation of the siladicyclopentadienyl ring, the metal atoms in **3–5** exhibit distorted tetrahedral configurations with the two chloride atoms. DFT calculations established that the size of the bridge ring influenced the catalytic activity. Thus, the catalytic activity of the *ansa*-titanocene complexes was remarkably enhanced by the silacycloalkyl bridge due to their increased conformational stability (14 × 10³ kg PE mol_{cat}⁻¹ h⁻¹ for **3c**). In addition, polyethylenes with high molecular weight such as M_w = (1.3–2.6) × 10⁶ (M_w/M_n = 1.6–2.0 by GPC) were obtained with **3**.

Introduction

The preparation of new types of *ansa*-metallocene complexes containing various bridged groups that introduce new internal interactions into the metallocene structure is without doubt of interest because of their high activity and stereospecificity in olefin polymerization.^{1,2} In fact, *ansa*-metallocene complexes containing various types of ring-bridging groups have been developed, and their ability to catalyze olefin polymerization has been assessed.^{3,4} At present, work on these systems is principally directed toward the elucidation of the relationship between the bridged ligand structure of the *ansa*-metallocene complexes and their catalytic activity.

We have recently demonstrated that diamido titanium(IV) complexes of the type (cyclo)Si(NBu)₂TiCl with silacycloalkyl-bridged ring structures display variable conformational stability depending on the size of the

ring.⁵ Owing to the cyclic silicon bridge, the silicon group can influence the metal center and greatly affect its chemical and catalytic activity. Compared with the four- or five-membered cyclic silicon bridge, the six-membered silicon bridge group is exceedingly stable. Therefore, the six-membered cyclic silicon-bridged complex is more

(2) Single-silicon bridged: (a) Antinolo, A.; Lopez-Solera, I.; Orive, I.; Otero, A.; Prashar, S.; Rodriguez, A. M.; Villasenor, E. *Organometallics* **2001**, *20*, 71. (b) Muller, C.; Lilje, D.; Kristen, M. O.; Jutz, P. *Angew. Chem., Int. Ed.* **2000**, *39*, 789. (c) Schumann, H.; Zietzke, K.; Weimann, R.; Demtschuk, J.; Kaminsky, W.; Schauwienold, A.-M. *J. Organomet. Chem.* **1999**, *574*, 228. (d) Alt, H. G.; Jung, M.; Milius, W. *J. Organomet. Chem.* **1998**, *558*, 111. (e) Suzuki, N.; Mise, T.; Yamaguchi, Y.; Chihara, T.; Ikegami, Y.; Ohmori, H.; Matsumoto, A.; Wakatsuki, Y. *J. Organomet. Chem.* **1998**, *560*, 47. (f) Obora, Y.; Stern, C. L.; Marks, T. J.; Nickias. *Organometallics* **1997**, *16*, 2503. (g) Herzog, T. A.; Zubris, D. T.; Bercaw, J. E. *J. Am. Chem. Soc.* **1996**, *118*, 11988. (h) Chen, Y.-X.; Rausch, M. D.; Chien, J. C. W. *J. Organomet. Chem.* **1995**, *497*, 1. (i) Giardello, M. A.; Eisen, M. S.; Stern, C. L.; Marks, T. J. *J. Am. Chem. Soc.* **1995**, *117*, 12114. (j) Stehling, U.; Diebold, U. J.; Kirsten, R.; Roll, W.; Brintzinger, H. H. *Organometallics* **1994**, *13*, 964. (k) Spaleck, W.; Kuber, F.; Winter, A.; Rohrmann, J.; Bachmann, B.; Antberg, M.; Dolle, V.; Paulus, E. F. *Organometallics* **1994**, *13*, 954. (l) Giardello, M. A.; Eisen, M. S.; Stern, C. L.; Marks, T. J. *J. Am. Chem. Soc.* **1993**, *115*, 3326. (m) Spaleck, W.; Antberg, M.; Rohrmann, J.; Winter, A.; Bachmann, B.; Kiprof, P.; Behm, J.; Herrmann, W. A. *Angew. Chem., Int. Ed. Engl.* **1992**, *31*, 1347. (n) Ewen, J. A.; Elder, M. J.; Jones, R. L.; Haspeslagh, L.; Atwood, J. L.; Bott, S. G.; Robinson, K. *Makromol. Chem. Macromol. Symp.* **1991**, *48/49*, 253. (o) Herrmann, W. A.; Rohrmann, J.; Herdtweck, E.; Spaleck, W.; Winter, A. *Angew. Chem., Int. Ed. Engl.* **1989**, *28*, 1511. (p) Mise, T.; Miya, S.; Yamazaki, H. *Chem. Lett.* **1989**, 1853.

(3) (a) Coates, G. W. *Chem. Rev.* **2000**, *100*, 1223. (b) Resconi, L.; Cavallo, L.; Fait, A.; Piemontesi, F. *Chem. Rev.* **2000**, *100*, 1253. (c) Brinzingler, H. H.; Fischer, D.; Mülhaupt, R.; Rieger, B.; Waymouth, R. M. *Angew. Chem., Int. Ed. Engl.* **1995**, *34*, 1143. (d) Mohring, P. C.; Coville, N. J. *J. Organomet. Chem.* **1994**, *20*, 257. (e) Kaminsky Catal. *Today* **1994**, *20*, 257. (f) Halterman, R. L. *Chem. Rev.* **1992**, *92*, 965. (g) Jordan, R. F. *Adv. Organomet. Chem.* **1991**, *32*, 325.

[†] Korea University.

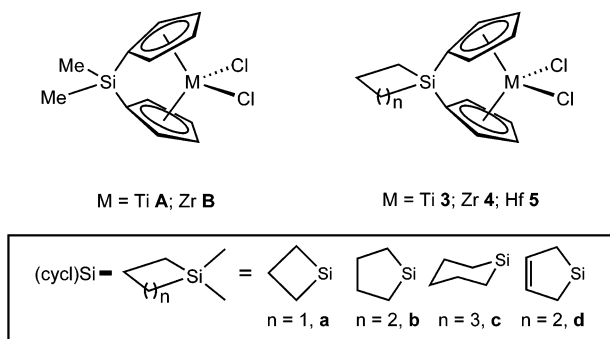
[‡] Hanbat National University.

[§] Ajou University.

[‡] Kyung Hee University.

(1) Single-carbon bridged: (a) Alt, H.; Köppl, A. *Chem. Rev.* **2000**, *100*, 1205. (b) Veghini, D.; Henling, L. M.; Burkhardt, T. J.; Bercaw, J. E. *J. Am. Chem. Soc.* **1999**, *121*, 564. (c) Ewen, J. A.; Jones, R. L.; Elder, M. J.; Rheingold, A. L.; Liable-Sands, L. M. *J. Am. Chem. Soc.* **1998**, *120*, 10786. (d) Yoon, S. C.; Han, T. K.; Woo, B. W.; Song, H.; Woo, S. I.; Park, J. T. *J. Organomet. Chem.* **1997**, *534*, 81. (e) Green, M. L. H.; Ishihara, N. *J. Chem. Soc., Dalton Trans.* **1994**, 657. (f) Razavi, A.; Atwood, J. L. *J. Organomet. Chem.* **1995**, *497*, 105. (g) Llinas, G. H.; Day, R. O.; Rausch, M. D.; Chien, J. C. W. *Organometallics* **1993**, *12*, 1283. (h) Razavi, A.; Atwood, J. L. *J. Organomet. Chem.* **1993**, *459*, 117. (i) Razavi, A.; Ferrara, J. *J. Organomet. Chem.* **1992**, *435*, 299. (j) Ewen, J. A.; Jones, R. L.; Razavi, A.; Ferrara, J. D. *J. Am. Chem. Soc.* **1988**, *110*, 6255.

Chart 1

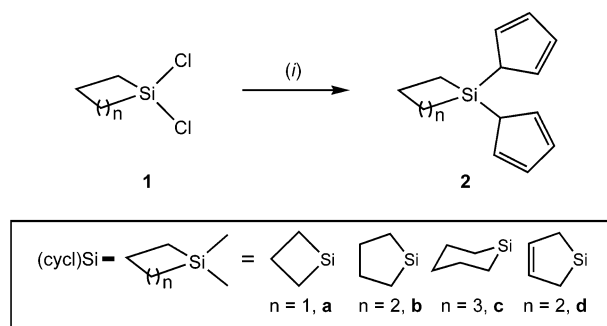


likely to be stable in *ansa*-metallocene complexes, due to conformational effects caused by the stable six-membered silicon ring. Conformational stability is likely to have a significant effect on catalytic activity.

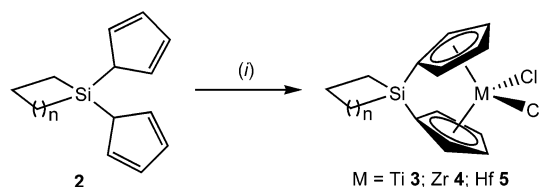
To date, only a few group IV *ansa*-metallocene complexes with a cyclic silicon bridge have been synthesized, including those with silacyclobutyl and silacyclopentyl groups. The first silacycloalkyl-bridged *ansa*-metallocene complexes to be synthesized were *rac*- and *meso*-(CH₂)₄Si(C₉H₆)₂ZrCl₂ and *rac*-(CH₂)₄Si(C₉H₁₀)₂ZrCl₂.⁶ Those *ansa*-metallocene complexes were used to catalyze the copolymerization of ethylene and propylene. A detailed description of these metallocene-catalyzed polymerizations is given by Tsai and Chien.⁷ Rausch and Chien subsequently reported silacyclobutane-bridged *ansa*-metallocene complexes, *rac*- and *meso*-(CH₂)₃Si(C₉H₆)₂ZrCl₂, and studied their catalysis of ethylene and propylene polymerization.⁸ However, thus far there has been no systematic study on the catalytic behavior of *ansa*-metallocene complexes as a function of the bridge ring size. On the basis of our earlier work on silacycloalkyl-bridged diamido group IV metal complexes, herein we report the synthesis, crystal structures, and catalytic behavior of silacycloalkyl-bridged *ansa*-metallocene complexes **3–5**. The results of the present study reveal that the inclusion of the silacycloalkyl bridge remarkably enhances the catalytic activity of *ansa*-metallocene complexes and promotes the formation of very high molecular weight polyethylene. The results additionally show the following trend in the catalytic activity of silacycloalkyl-bridged *ansa*-metallocene complexes: silacyclobutyl < silacyclopentyl ≈ silacyclopentyl < silacyclohexyl.

Results and Discussions

Synthesis of 1,1-Dicyclopentadienyl-1-Silacycloalkane or -alkene (2). Chelating dicyclopentadienes with silyl substituents (**2**) are readily accessible

Scheme 1^a

^a Conditions: (i) 2 LiCp, THF, 25 °C.

Scheme 2^a

^a Conditions: (i) (a) 2 BuⁿLi, THF, -78 °C; (b) MCl₄ (M = Ti, Zr, Hf), THF, -78 °C.

by the reaction of lithium cyclopentadiene with 1,1-dichloro-1-silacycloalkane or -alkene (**1**). Compounds **2** are therefore readily accessible by a procedure analogous to that used for the synthesis of the dimethylsilyldicyclopentadiene (Me)₂SiCp₂.² For example, the reaction of cyclopentadiene with *n*-butyllithium followed by the addition of **1** gives 1,1-dicyclopentadienyl-1-silacycloalkane or -alkene (**2**) in good yield (Scheme 1). The lithium salts of the bidentate dicyclopentadienes (**2**) were used as the starting materials for the synthesis of the *ansa*-metallocene complexes (**3–5**).

Synthesis of *ansa*-Metallocene Complexes (3–5**).** The *ansa*-metallocene complexes [{η⁵:η⁵-Cp₂-(cycl)-Si}MCl₂] (M = Ti (**3**), Zr (**4**), Hf (**5**)) were synthesized by the reaction of [{η⁵:η⁵-Cp₂-(cycl)Si}Li₂] (**2**) with MCl₄ (Scheme 2). The reaction of MCl₄ (1.0 mmol) and the dilithium salt of **2** (1 equiv) in diethyl ether afforded **3–5** in good yield (38–71%). Compounds **3–5** were obtained as air-sensitive crystals by low-temperature recrystallization from pentane. Satisfactory elemental analyses were obtained for **3–5**, and the ¹H and ¹³C NMR spectral data were consistent with the presence of the bidentate cyclic silyldicyclopentadiene (see Experimental Section).

The ¹H NMR spectra of **3–5** (Table 1) show two multiplets for the α and β cyclopentadienyl ring protons corresponding to the AA'BB' system and broad overlapping multiplets for the methylene groups of the silacycloalkyl bridging unit. The differences (Δδ) of the chemical shifts between the α-H and β-H of the cyclopentadienyl ring (Cp) decrease with increasing atomic number of the metal. Thus, the ¹H NMR signals for Cp in **3–5** are downfield of those for the free Cp. This can be explained on the basis of a tetrahedral geometry for the cyclopentadiene and chloride units and evidence of Ti–Cp coordination in solution and is consistent with similar findings for the siladicyclopentadienyl ring in Me₂SiCp₂MCl₂ (M = Ti **A**; Zr **B**).^{9,10} The reaction proceeds with high yield and gives preferential forma-

(4) (a) Tian, G.; Wang, B.; Xu, S.; Zhang, Y.; Zhou, X. *J. Organomet. Chem.* **1999**, *579*, 24. (b) Spaleck, W.; Kuber, F.; Winter, A.; Rohrmann, J.; Bachmann, B.; Antberg, M.; Dolle, V.; Paulus, E. F. *Organometallics* **1994**, *13*, 954. (c) Hermann, W.; Rohrmann, J.; Herdtweck, E.; Spaleck, W.; Winter, A. *Angew. Chem., Int. Ed. Engl.* **1989**, *11*, 28.

(5) (a) Kim, S.-J.; Jung, I. N.; Yoo, B. R.; Cho, S.; Ko, J.; Kim, S. H.; Kang, S. O. *Organometallics* **2001**, *20*, 1501. (b) Kim, S.-J.; Jung, I. N.; Yoo, B. R.; Cho, S.; Ko, J.; Kim, S. H.; Byun, D.; Kang, S. O. *Organometallics* **2001**, *20*, 2136.

(6) Luttikhedde, H. J. G.; Leino, R. P.; Näsman, J. H.; Ahlgrén, M.; Pakkanen, T. *J. Organomet. Chem.* **1995**, *486*, 193.

(7) Tsai, W.-M.; Chien, J. C. W. *J. Polym. Sci. Part A Polym. Chem.* **1994**, *32*, 149.

(8) Chen, Y.-X.; Rausch, M. D.; Chien, J. C. W. *J. Organomet. Chem.* **1995**, *487*, 29.

Table 1. Key Spectral Data of Compounds

| compd | ¹ H | assignment | ¹³ C{ ¹ H} | assignment | yield (%) | compd | ¹ H | assignment | ¹³ C{ ¹ H} | assignment | yield (%) |
|-----------|----------------|---|----------------------------------|--|-----------|-----------|---------------------|---|----------------------------------|--|-----------|
| 2a | 1.20 | (m, 4H, SiCH ₂) | 15.76 | (SiCH ₂) | 62 | 2b | 1.15 | (m, 4H, SiCH ₂) | 8.44 | (SiCH ₂) | 54 |
| | 1.74 | (m, 2H, CH ₂ CH ₂) | 21.02 | (CH ₂ CH ₂) | | | 1.77 | (m, 4H, CH ₂ CH ₂) | 24.95 | (CH ₂ CH ₂) | |
| | 6.48 | (m, 4H, C ₅ H ₄) | | | | | 6.45 | (m, 4H, C ₅ H ₄) | | | |
| 2c | 0.91 | (m, 4H, SiCH ₂) | 11.82 | (SiCH ₂) | 64 | 2d | 0.90 | (m, 4H, SiCH ₂) | 12.99 | (SiCH ₂) | 44 |
| | 1.46 | (m, 2H, CH ₂ CH ₂ CH ₂) | 24.34 | (CH ₂ CH ₂) | | | 5.70 | (m, 2H, =CH) | 131.86 | (=CH ₂) | |
| | 1.75 | (m, 4H, CH ₂ CH ₂) | 31.96 | (CH ₂ CH ₂ CH ₂) | | | 6.64 | (m, 4H, C ₅ H ₄) | | | |
| | 6.45 | (m, 4H, C ₅ H ₄) | | | | | | | | | |
| 3a | 1.77 | (m, 4H, SiCH ₂) | 13.89 | (SiCH ₂) | 38 | 3b | 1.28 | (m, 4H, SiCH ₂) | 9.37 | (SiCH ₂) | 46 |
| | 2.49 | (m, 2H, CH ₂ CH ₂) | 26.79 | (CH ₂ CH ₂) | | | 1.92 | (m, 4H, CH ₂ CH ₂) | 26.55 | (CH ₂ CH ₂) | |
| | 6.04 | (m, 2H, C ₅ H ₄) | 105.48 | (<i>ipso</i> -C ₅ H ₄) | | | 5.98 | (m, 2H, C ₅ H ₄) | 105.12 | (<i>ipso</i> -C ₅ H ₄) | |
| | 7.23 | (m, 2H, C ₅ H ₄) | 119.25 | (C ₅ H ₄) | | | 7.23 | (m, 2H, C ₅ H ₄) | 119.49 | (C ₅ H ₄) | |
| 3c | 1.31 | (m, 4H, SiCH ₂) | 9.03 | (SiCH ₂) | 65 | 3d | 1.52 | (m, 4H, SiCH ₂) | 13.94 | (SiCH ₂) | 58 |
| | 1.64 | (m, 2H, CH ₂ CH ₂ CH ₂) | 23.76 | (CH ₂ CH ₂) | | | 5.86 | (m, 2H, =CH) | 105.53 | (<i>ipso</i> -C ₅ H ₄) | |
| | 1.96 | (m, 4H, CH ₂ CH ₂) | 29.48 | (CH ₂ CH ₂ CH ₂) | | | 6.02 | (m, 2H, C ₅ H ₄) | 119.34 | (C ₅ H ₄) | |
| | 5.98 | (m, 2H, C ₅ H ₄) | 105.54 | (<i>ipso</i> -C ₅ H ₄) | | | 7.24 | (m, 2H, C ₅ H ₄) | 131.37 | (=CH ₂) | |
| | 7.22 | (m, 2H, C ₅ H ₄) | 119.06 | (C ₅ H ₄) | | | | | 135.62 | (C ₅ H ₄) | |
| 4a | 0.90 | (m, 4H, SiCH ₂) | 14.38 | (SiCH ₂) | 46 | 4b | 1.28 | (m, 4H, SiCH ₂) | 9.76 | (SiCH ₂) | 40 |
| | 1.35 | (m, 2H, CH ₂ CH ₂) | 25.48 | (CH ₂ CH ₂) | | | 1.91 | (m, 4H, CH ₂ CH ₂) | 26.60 | (CH ₂ CH ₂) | |
| | 5.98 | (m, 2H, C ₅ H ₄) | 105.48 | (<i>ipso</i> -C ₅ H ₄) | | | 6.01 | (m, 2H, C ₅ H ₄) | 108.03 | (<i>ipso</i> -C ₅ H ₄) | |
| | 7.22 | (m, 2H, C ₅ H ₄) | 119.70 | (C ₅ H ₄) | | | 6.98 | (m, 2H, C ₅ H ₄) | 115.05 | (C ₅ H ₄) | |
| | | | 135.88 | (C ₅ H ₄) | | | | | 128.69 | (C ₅ H ₄) | |
| 4c | 1.32 | (m, 4H, SiCH ₂) | 9.26 | (SiCH ₂) | 48 | 4d | 1.32 | (m, 4H, SiCH ₂) | 14.55 | (SiCH ₂) | 45 |
| | 1.63 | (m, 2H, CH ₂ CH ₂ CH ₂) | 23.66 | (CH ₂ CH ₂) | | | 6.05 | (m, 2H, C ₅ H ₄) | 107.38 | (<i>ipso</i> -C ₅ H ₄) | |
| | 1.95 | (m, 4H, CH ₂ CH ₂) | 29.57 | (CH ₂ CH ₂ CH ₂) | | | 6.14 | (m, 2H, =CH) | 114.87 | (C ₅ H ₄) | |
| | 5.99 | (m, 2H, C ₅ H ₄) | 108.29 | (<i>ipso</i> -C ₅ H ₄) | | | 7.00 | (m, 2H, C ₅ H ₄) | 128.75 | (C ₅ H ₄) | |
| | 6.97 | (m, 2H, C ₅ H ₄) | 114.52 | (C ₅ H ₄) | | | | | 130.45 | (=CH ₂) | |
| 5a | 1.75 | (m, 4H, SiCH ₂) | 14.21 | (SiCH ₂) | 66 | 5b | 1.28 | (m, 4H, SiCH ₂) | 9.71 | (SiCH ₂) | 73 |
| | 2.49 | (m, 2H, CH ₂ CH ₂) | 18.43 | (CH ₂ CH ₂) | | | 1.92 | (m, 4H, CH ₂ CH ₂) | 26.61 | (CH ₂ CH ₂) | |
| | 5.98 | (m, 2H, C ₅ H ₄) | 97.83 | (<i>ipso</i> -C ₅ H ₄) | | | 5.93 | (m, 2H, C ₅ H ₄) | 98.43 | (<i>ipso</i> -C ₅ H ₄) | |
| | 6.89 | (m, 2H, C ₅ H ₄) | 112.97 | (C ₅ H ₄) | | | 6.88 | (m, 2H, C ₅ H ₄) | 113.00 | (C ₅ H ₄) | |
| | | | 127.54 | (C ₅ H ₄) | | | | | 127.73 | (C ₅ H ₄) | |
| 5c | 1.35 | (m, 4H, SiCH ₂) | 9.32 | (SiCH ₂) | 71 | 5d | 2.02 | (m, 4H, SiCH ₂) | 26.00 | (SiCH ₂) | 66 |
| | 1.63 | (m, 2H, CH ₂ CH ₂ CH ₂) | 23.75 | (CH ₂ CH ₂) | | | 5.97 | (m, 2H, C ₅ H ₄) | 97.61 | (<i>ipso</i> -C ₅ H ₄) | |
| | 1.95 | (m, 4H, CH ₂ CH ₂) | 26.64 | (CH ₂ CH ₂ CH ₂) | | | 6.13 | (m, 2H, =CH) | 112.65 | (C ₅ H ₄) | |
| | 5.92 | (m, 2H, C ₅ H ₄) | 98.33 | (<i>ipso</i> -C ₅ H ₄) | | | 6.89 | (m, 2H, C ₅ H ₄) | 127.78 | (C ₅ H ₄) | |
| | 6.87 | (m, 2H, C ₅ H ₄) | 112.49 | (C ₅ H ₄) | | | | | 130.25 | (=CH ₂) | |
| 6a | -0.11 | (m, 6H, TiCH ₃) | 14.37 | (SiCH ₂) | | 6b | -0.07 | (m, 6H, TiCH ₃) | 9.33 | (SiCH ₂) | |
| | 0.88 | (m, 4H, SiCH ₂) | 26.62 | (CH ₂ CH ₂) | | | 0.91 | (m, 4H, SiCH ₂) | 26.48 | (CH ₂ CH ₂) | |
| | 1.09 | (m, 2H, CH ₂ CH ₂) | 45.24 | (TiCH ₃) | | | 1.75 | (m, 4H, CH ₂ CH ₂) | 45.11 | (TiCH ₃) | |
| | 5.54 | (m, 2H, C ₅ H ₄) | 100.77 | (<i>ipso</i> -C ₅ H ₄) | | | 5.54 | (m, 2H, C ₅ H ₄) | 100.01 | (<i>ipso</i> -C ₅ H ₄) | |
| | 7.22 | (m, 2H, C ₅ H ₄) | 115.92 | (C ₅ H ₄) | | | 7.25 | (m, 2H, C ₅ H ₄) | 115.76 | (C ₅ H ₄) | |
| 6c | -0.10 | (m, 6H, TiCH ₃) | 9.35 | (SiCH ₂) | | 6d | -0.06 | (m, 6H, TiCH ₃) | 14.23 | (SiCH ₂) | |
| | 0.91 | (m, 4H, SiCH ₂) | 23.79 | (CH ₂ CH ₂) | | | 1.63 | (m, 4H, SiCH ₂) | 45.39 | (TiCH ₃) | |
| | 1.49 | (m, 2H, CH ₂ CH ₂ CH ₂) | 29.80 | (CH ₂ CH ₂ CH ₂) | | | 5.82 | (m, 2H, C ₅ H ₄) | 99.84 | (<i>ipso</i> -C ₅ H ₄) | |
| | 1.80 | (m, 4H, CH ₂ CH ₂) | 44.87 | (TiCH ₃) | | | 6.04 | (m, 2H, =CH) | 115.67 | (C ₅ H ₄) | |
| | 5.54 | (m, 2H, C ₅ H ₄) | 100.36 | (<i>ipso</i> -C ₅ H ₄) | | | 7.34 | (m, 2H, C ₅ H ₄) | 125.48 | (C ₅ H ₄) | |
| | | 115.40 | (C ₅ H ₄) | | | 131.18 | (=CH ₂) | | | | |
| | | 125.24 | (C ₅ H ₄) | | | | | | | | |

tion of the tetrahedral *ansa*-metallocene complexes. In addition, the increased kinetic stability of products **3**–**5** compared to that of **A** and **B** is most likely a consequence of the formation of a *spiro* ring that is imposed by the cyclic silyl backbone.

The X-ray crystallographic analysis of *ansa*-metallocene complex **3b** revealed the expected structure, shown in Figure 1. The asymmetric unit contains two independent molecules with almost identical structures. Selected bond distances and angles are summarized in Tables 3 and 4. In the solid state, the titanium atom is coordinated by the η⁵-cyclopentadienyl fragments of two *ansa*-type ligands and two chlorine atoms. The molecule

has noticeable distortions due to the silacyclopentyl bridge between two cyclopentadienyl fragments. The C(5)–Si(1)–C(10) angle (90.4(3)°) is significantly less than the tetrahedral value (109.5°). The angle between the normal to the Cp plane and the line from the titanium atom to the centroid of the Cp ring is 2.69° for the C(5)···C(9) ring and 1.62° for the C(10)···C(14) ring. The Si(1) atom is displaced from the planes of the two Cp units toward Ti(1) by 0.54(1) and 0.57(1) Å; the angle between the planes of the Cp rings is 55.7(3)°. The Ti–C(Cp) distances are not equal for both Cp rings. The Ti(1)–C(5) and Ti(1)–C(10) bonds (2.368(6) and 2.373(7) Å) are the shortest, whereas similar bonds with C(7), C(8), C(12), and C(13) atoms (2.439(7), 2.436(7), 2.411(7), and 2.424(7) Å, respectively) are the longest in the molecule. The Ti(1)–Cl(1) and Ti(1)–Cl(2) bond lengths (2.343(2), and 2.355(2) Å) and the angle between

(9) Davis, J. H.; Sun, H.; Redfield, D.; Stucky, G. D. *J. Magn. Reson.* **1980**, *37*, 441.

(10) Smith, J. A.; Seyere, J. V.; Huttner, G.; Brintzinger, H. H. *J. Organomet. Chem.* **1979**, *173*, 175.

Table 2. X-ray Crystallographic Data and Processing Parameters for Compounds **3b**, **3c**, **4b**, and **4c**

| | 3b | 3c | 4b | 4c |
|--|---|---|--|--|
| formula | C ₂₈ H ₃₂ Cl ₄ Si ₂ Ti ₂ | C ₃₀ H ₃₆ Cl ₄ Si ₂ Ti ₂ | C ₁₄ H ₁₆ Cl ₂ SiZr | C ₁₅ H ₁₈ Cl ₂ SiZr |
| fw | 662.32 | 690.37 | 374.48 | 388.50 |
| cryst class | triclinic | triclinic | monoclinic | triclinic |
| space group | <i>P</i> 1 | <i>P</i> 1 | <i>P</i> 2 ₁ / <i>c</i> | <i>P</i> 1 |
| <i>Z</i> | 2 | 2 | 4 | 2 |
| cell constants | | | | |
| <i>a</i> , Å | 9.9801(6) | 10.3423(8) | 7.3803(7) | 7.5881(2) |
| <i>b</i> , Å | 11.948(1) | 11.557(1) | 24.012(1) | 8.7191(2) |
| <i>c</i> , Å | 12.527(1) | 13.196(2) | 8.5569(5) | 12.985(2) |
| α , deg | 99.094(7) | 97.43(1) | | 91.47(1) |
| β , deg | 89.986(6) | 89.85(1) | 102.226(6) | 106.22(2) |
| γ , deg | 102.845(6) | 102.199(7) | | 104.86(2) |
| <i>V</i> , Å ³ | 1437.1(2) | 1528.1(3) | 1482.0(2) | 792.8(3) |
| μ , mm ⁻¹ | 1.029 | 0.971 | 1.162 | 1.090 |
| cryst size, mm | 0.25 × 0.3 × 0.35 | 0.3 × 0.3 × 0.45 | 0.35 × 0.4 × 0.45 | 0.2 × 0.35 × 0.35 |
| <i>d</i> _{calcd.} , g/cm ³ | 1.531 | 1.500 | 1.678 | 1.627 |
| <i>F</i> (000) | 680 | 712 | 752 | 392 |
| radiation | Mo K α (λ = 0.7107), <i>T</i> = 293 K | | | |
| θ range, deg | 1.65 to 25.97 | 1.56 to 25.97 | 1.70 to 25.96 | 1.64 to 25.97 |
| <i>h</i> , <i>k</i> , <i>l</i> collected | +12, \pm 14, \pm 15 | +12, \pm 14, \pm 16 | +9, +29, \pm 10 | +9, \pm 10, \pm 15 |
| no. of reflns meads | 6014 | 6368 | 3124 | 3431 |
| no. of unique reflns | 5632 | 5981 | 2897 | 3107 |
| no. of reflns used in refinement (<i>I</i> > 2 σ (<i>I</i>)) | 5629 | 5978 | 2872 | 3107 |
| no. of params | 341 | 359 | 171 | 180 |
| <i>R</i> ₁ ^a | 0.054 | 0.090 | 0.052 | 0.050 |
| <i>wR</i> ₂ ^a | 0.129 | 0.190 | 0.225 | 0.126 |
| GOF | 0.92 | 1.01 | 1.87 | 1.05 |

^a $R_1 = \sum ||F_o| - |F_c||$ (based on reflections with $F_o^2 > 2\sigma(F_o^2)$). ^b $wR_2 = [\sum [w(F_o^2 - F_c^2)^2] / \sum [w(F_o^2)^2]]^{1/2}$; $w = 1/[\sigma^2(F_o^2) + (0.095P)^2]$; $P = [\max(F_o^2, 0) + 2F_c^2]/3$ (also with $F_o^2 > 2\sigma(F_o^2)$).

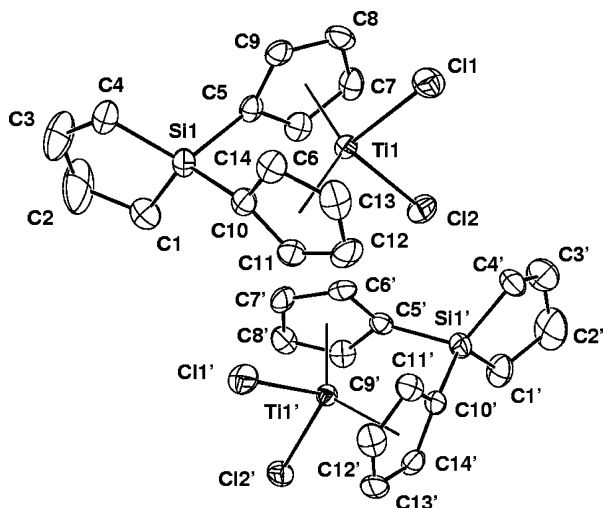


Figure 1. Molecular structure of **3b** with thermal ellipsoids drawn at the 30% level.

these bonds, Cl(1)–Ti(1)–Cl(2) (96.32(8)°), in the structure have the standard values. The silacyclopentane ring is slightly distorted from planarity with a maximum deviation of 0.089(6)°. All of the silacyclopentane bond lengths and bond angles are close to the standard values. The molecular structure of **3c** is presented in Figure 2. The asymmetric unit contains two independent, chemically identical molecules of **3c**. Despite the change in the bridge silacycloalkyl unit, titanocene **3c** has structural parameters similar to those found in **3b**.

The structures of *ansa*-zirconocene complexes **4b** and **4c** were confirmed by X-ray crystallographic analysis (Figures 3 and 4). In both complexes the zirconium atom is pseudotetrahedrally coordinated by the two Cp groups of the 1,1-dicyclopentadienyl-1-silacyclopentane or -hexane unit and the two chloride atoms. For molecule **4b**, the centroid of one Cp ring lies in the plane defined by

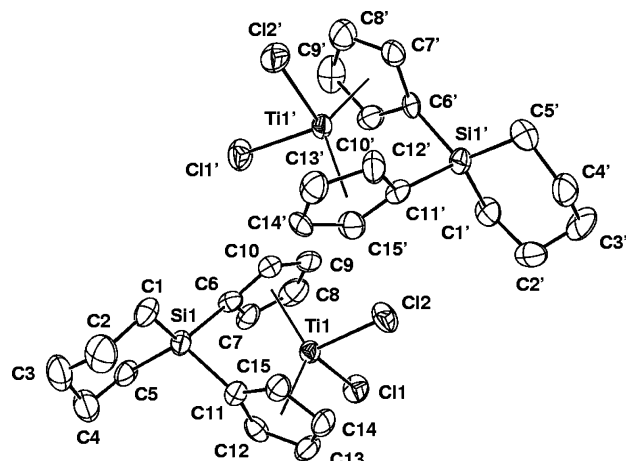


Figure 2. Molecular structure of **3c** with thermal ellipsoids drawn at the 30% level.

the Si(1), C(5), and C(10) atoms [the distances of the centroids of Cp(1) and Cp(2) (Cp(1) = C(5)–C(9), Cp(2) = C(10)–C(14)) to the plane are approximately 0.016 and 0.002 Å, respectively], and the Zr atom is located out of this plane by approximately 0.01(2) Å. For molecule **4c**, the Si(1)–C(6)–C(11) plane contains the centroids of both Cp rings [Cp(1) and Cp(2) distances to the plane are approximately 0.024 and 0.008 Å], and the Zr atom is located out of this plane by approximately 0.011(9) Å. The dihedral angle between the Si(1)–C(5)–C(10) or Si(1)–C(6)–C(11) plane and the Cp(1)–Zr(1)–Cp(2) plane is almost the same (0.22° and 0.51° for **4b** and **4c**, respectively). Another geometrical feature of the molecule is the plane Zr(1)–Cl(1)–Cl(2), which contains the Si(1) atom of the silacycloalkyl bridge. This bridge [Si(1)–C(5)–C(10) or Si(1)–C(6)–C(11), approximately 94°] constrains the bent metallocene geometry in such a way that the distances from the zirconium to the carbons of the cyclopentadienyl rings are different

Table 3. Selected Interatomic Distances (Å)

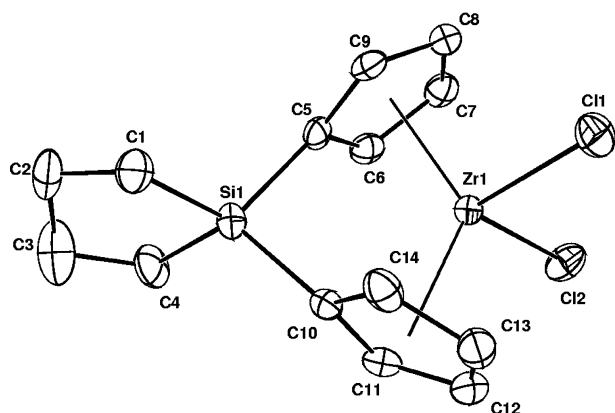
| Compound 3b | | | | | | | | | |
|--------------------|----------|---------------|----------|---------------|----------|---------------|----------|---------------|----------|
| Ti(1)–Cl(1) | 2.343(2) | Ti(1)–Cl(2) | 2.355(2) | Si(1)–C(1) | 1.856(8) | Si(1)–C(4) | 1.856(8) | Si(1)–C(5) | 1.861(7) |
| Si(1)–C(10) | 1.869(7) | Ti(1')–Cl(1') | 2.344(2) | Ti(1')–Cl(2') | 2.349(2) | Si(1')–C(1') | 1.860(9) | Si(1')–C(4') | 1.853(8) |
| Si(1')–C(5') | 1.858(7) | Si(1')–C(10') | 1.862(7) | Ti(1)–C(5) | 2.368(6) | Ti(1)–C(6) | 2.379(7) | Ti(1)–C(7) | 2.439(7) |
| Ti(1)–C(8) | 2.436(7) | Ti(1)–C(9) | 2.339(7) | Ti(1)–C(10) | 2.373(7) | Ti(1)–C(11) | 2.367(7) | Ti(1)–C(12) | 2.411(7) |
| Ti(1)–C(13) | 2.424(7) | Ti(1)–C(14) | 2.349(7) | Ti(1')–C(5') | 2.374(7) | Ti(1')–C(6') | 2.349(7) | Ti(1')–C(7') | 2.448(7) |
| Ti(1')–C(8') | 2.438(7) | Ti(1')–C(9') | 2.386(7) | Ti(1')–C(10') | 2.376(7) | Ti(1')–C(11') | 2.364(7) | Ti(1')–C(12') | 2.413(7) |
| Ti(1')–C(13') | 2.424(7) | Ti(1')–C(14') | 2.369(7) | | | | | | |
| Compound 3c | | | | | | | | | |
| Ti(1)–Cl(1) | 2.345(4) | Ti(1)–Cl(2) | 2.340(4) | Si(1)–C(1) | 1.85(1) | Si(1)–C(5) | 1.85(1) | Si(1)–C(6) | 1.87(1) |
| Si(1)–C(11) | 1.88(1) | Ti(1')–Cl(1') | 2.343(4) | Ti(1')–Cl(2') | 2.341(4) | Si(1')–C(1') | 1.84(1) | Si(1')–C(5') | 1.86(1) |
| Si(1')–C(6') | 1.87(1) | Si(1')–C(11') | 1.86(1) | Ti(1)–C(6) | 2.37(1) | Ti(1)–C(7) | 2.36(1) | Ti(1)–C(8) | 2.40(2) |
| Ti(1)–C(9) | 2.41(1) | Ti(1)–C(10) | 2.36(1) | Ti(1)–C(11) | 2.37(1) | Ti(1)–C(12) | 2.34(1) | Ti(1)–C(13) | 2.44(1) |
| Ti(1)–C(14) | 2.44(1) | Ti(1)–C(15) | 2.37(1) | Ti(1')–C(6') | 2.37(1) | Ti(1')–C(7') | 2.37(1) | Ti(1')–C(8') | 2.41(2) |
| Ti(1')–C(9') | 2.43(1) | Ti(1')–C(10') | 2.34(1) | Ti(1')–C(11') | 2.36(1) | Ti(1')–C(12') | 2.38(1) | Ti(1')–C(13') | 2.43(1) |
| Ti(1')–C(14') | 2.44(1) | Ti(1')–C(15') | 2.35(1) | | | | | | |
| Compound 4b | | | | | | | | | |
| Zr(1)–Cl(1) | 2.438(2) | Zr(1)–Cl(2) | 2.429(2) | Si(1)–C(1) | 1.860(9) | Si(1)–C(4) | 1.879(8) | Si(1)–C(5) | 1.878(7) |
| Si(1)–C(10) | 1.866(8) | Zr(1)–C(5) | 2.488(7) | Zr(1)–C(6) | 2.469(7) | Zr(1)–C(7) | 2.562(8) | Zr(1)–C(8) | 2.543(8) |
| Zr(1)–C(9) | 2.481(7) | Zr(1)–C(10) | 2.486(7) | Zr(1)–C(11) | 2.480(8) | Zr(1)–C(12) | 2.530(9) | Zr(1)–C(13) | 2.546(8) |
| Zr(1)–C(14) | 2.489(8) | | | | | | | | |
| Compound 4c | | | | | | | | | |
| Zr(1)–Cl(1) | 2.435(1) | Zr(1)–Cl(2) | 2.440(1) | Si(1)–C(1) | 1.848(5) | Si(1)–C(5) | 1.851(5) | Si(1)–C(6) | 1.862(5) |
| Si(1)–C(11) | 1.871(5) | Zr(1)–C(6) | 2.489(5) | Zr(1)–C(7) | 2.484(5) | Zr(1)–C(8) | 2.535(6) | Zr(1)–C(9) | 2.534(6) |
| Zr(1)–C(10) | 2.484(5) | Zr(1)–C(11) | 2.486(4) | Zr(1)–C(12) | 2.477(4) | Zr(1)–C(13) | 2.558(5) | Zr(1)–C(14) | 2.568(4) |
| Zr(1)–C(15) | 2.491(4) | | | | | | | | |

Table 4. Selected Interatomic Angles (deg)

| Compound 3b | | | | | |
|---------------------|----------|----------------------|----------|--------------------|----------|
| Cl(1)–Ti(1)–Cl(2) | 96.32(8) | C(1)–Si(1)–C(4) | 96.7(4) | C(1)–Si(1)–C(5) | 114.9(3) |
| C(5)–Si(1)–C(10) | 90.4(3) | Cl(1')–Ti(1')–Cl(2') | 96.03(8) | C(4')–Si(1')–C(1') | 97.4(4) |
| C(1')–Si(1')–C(10') | 120.4(4) | C(5')–Si(1')–C(10') | 91.0(3) | C(1)–Si(1)–C(10) | 120.5(4) |
| | | | | C(5')–Si(1')–C(1') | 113.9(4) |
| Compound 3c | | | | | |
| Cl(2)–Ti(1)–Cl(1) | 97.4(2) | C(1)–Si(1)–C(5) | 106.0(7) | C(1)–Si(1)–C(6) | 118.5(6) |
| C(6)–Si(1)–C(11) | 89.8(6) | Cl(2')–Ti(1')–Cl(1') | 98.2(2) | C(1')–Si(1')–C(5') | 108.0(6) |
| C(1')–Si(1')–C(11') | 113.5(6) | C(11')–Si(1')–C(6') | 90.4(5) | C(1)–Si(1)–C(11) | 112.9(6) |
| | | | | C(1')–Si(1')–C(6') | 114.5(6) |
| Compound 4b | | | | | |
| Cl(2)–Zr(1)–Cl(1) | 99.36(9) | C(1)–Si(1)–C(4) | 97.2(4) | C(1)–Si(1)–C(5) | 114.7(4) |
| C(10)–Si(1)–C(5) | 94.3(3) | | | C(1)–Si(1)–C(10) | 117.9(4) |
| Compound 4c | | | | | |
| Cl(2)–Zr(1)–Cl(1) | 97.71(5) | C(1)–Si(1)–C(5) | 106.1(2) | C(1)–Si(1)–C(6) | 116.8(2) |
| C(6)–Si(1)–C(11) | 94.0(2) | | | C(1)–Si(1)–C(11) | 111.4(2) |

[$d(\text{Zr}–\text{C})$ range 2.469(7)–2.562(8) Å; $d(\text{Zr}–\text{C})$ range 2.477(4)–2.568(4) Å], which forces the η^5 -coordination mode of the ligands toward a η^3 -coordination.

Overall the molecular parameters about the central metal atom are comparable to those reported for acyclic silicon-bridged metallocene complexes [SiMe₂(C₅H₄)₂]-MCl₂ (M = Ti **A**; Zr **B**).¹¹ In addition, it is noteworthy

**Figure 3.** Molecular structure of **4b** with thermal ellipsoids drawn at the 30% level.

that the geometrical features associated with the silacyclopentyl-bridged metallocene complexes (**3b** and **4b**) are similar to those of the corresponding silacyclohexyl-bridged metallocene complexes (**3c** and **4c**).

Table 5 lists selected geometric features of the crystallographically characterized silacycloalkyl- and dimethylsilyl-bridged *ansa*-metallocene complexes (**A** and **B**). The bite angle (γ) of the bridge, the dihedral angle (α) between the ring planes, and the angle (δ) formed

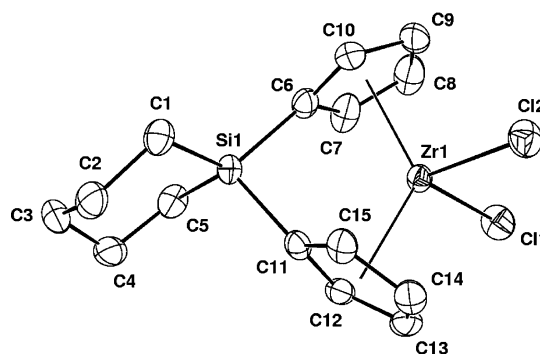
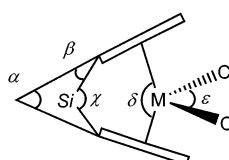
**Figure 4.** Molecular structure of **4c** with thermal ellipsoids drawn at the 30% level.

Table 5. Important Structural Parameters of 3b, 3c, 4b, and 4c

| | 3b | 3c | 4b | 4c |
|--|--------|--------|--------|--------|
| Si–Cp (Å) | 1.863 | 1.867 | 1.872 | 1.867 |
| Cp _{cent} –M (Å) | 2.069 | 2.072 | 2.201 | 2.205 |
| Si–M (Å) | 3.278 | 3.283 | 3.347 | 3.351 |
| C–Si–C (deg) | 97.05 | 107.25 | 97.21 | 106.12 |
| Cp(C)–Si–Cp(C) (deg) | 90.72 | 90.13 | 94.24 | 94.05 |
| Cp _{cent} –M–Cp _{cent} (deg) | 129.12 | 129.43 | 125.57 | 125.48 |
| Cl–M–Cl (deg) | 96.18 | 97.80 | 99.37 | 97.71 |

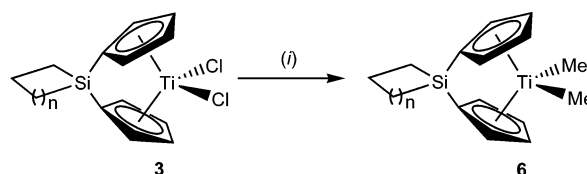
Table 6. Relationship between ansa-Metallocene Complexes Defining Angles of 3b, 3c, A, 4b, 4c, and B


| | α | β | γ | δ | ϵ |
|-----------|----------|---------|----------|----------|------------|
| 3b | 55.7(3) | 18.57 | 90.4(3) | 129.13 | 96.32(8) |
| 3c | 55.4(5) | 18.19 | 89.8(6) | 129.02 | 97.4(2) |
| A | 51.2 | | 89.5 | 128.7 | 95.75 |
| 4b | 59.1(3) | 18.50 | 94.3(3) | 132.57 | 99.36(9) |
| 4c | 59.3(2) | 17.90 | 94.0(2) | 125.48 | 97.71(5) |
| B | 56.8 | | 93.2 | 125.4 | 97.98 |

by the metal center and the ring centroids are defined in Table 6. A closer examination of the structural parameters associated with the cyclopentadienyl rings indicates that the introduction of the silacycloalkyl bridge has brought about a distinct structural change. The principal modification that arises when the cyclopentadienyl rings are linked together by a silacycloalkyl bridge is an alteration in the dihedral angle (α) of the rings. By comparison with the dimethylsilyl-bridged titanocene dichloride (**A**), it is apparent that the silacycloalkyl bridge in **3b** and **3c** produces large changes (4–5°) in the dihedral angle (α).

Synthesis of Dimethyl Derivatives of ansa-Titanocene Complexes, (cycl)SiCp₂TiMe₂ (6). Because dialkyl species are important precursors for active polyolefin catalysts, we synthesized the dimethyl derivatives of the ansa-titanocene complexes (**6**). Methylation of a diethyl ether solution of **3** (1.0 mmol) with MeMgBr (2.4 mmol) at room temperature for 2 h afforded high yields of **6** (65–87%) as pale yellow solids. The compositions of **6** were confirmed by elemental analyses. As expected, the ¹H NMR spectra of **6** are consistent with pseudo-C_{2v} symmetry. Characteristic ¹H and ¹³C NMR resonances of the Ti-Me groups were observed at around δ –0.1. The silylacycloalkyl groups exhibit unresolved multiplets between δ 0.8 and 1.8, and the signals for the α and β cyclopentadienyl ring protons are observed as two multiplets at around δ 5.5 and 7.2. Although the reaction produces the desired products almost quantitatively, as indicated by NMR spectroscopy, we failed to isolate analytically pure crystalline products. The products were isolated as sticky solids, which were difficult to recrystallize due to their high solubility in common organic solvent, even in pentane. The reaction of **6** with B(C₆F₅)₃ (1 equiv) was carried out at low temperature, but only intractable

(11) Bajgur, C. S.; Tikkanen, W. R.; Petersen, J. L. *Inorg. Chem.* **1985**, *24*, 2539.

Scheme 3^a

^a Conditions: (i) 2 MeMgBr, Et₂O, –78 °C.

product was obtained. The ionic species decomposed slowly to yield unidentifiable species at room temperature within several hours. Despite considerable efforts, attempts to isolate and characterize the decomposition product were unsuccessful.

The results of the polymerization of ethylene using **3–4**/methylaluminoxane (MAO) are shown in Table 7. To our surprise the silacycloalkyl-bridged titanocene complexes (**3**) exhibited remarkably higher activities than the corresponding zirconocene complexes (**4**) under the stated conditions (Table 7). In general, bridged or unbridged zirconocene complexes show much higher activities than titanocene complexes.¹² One explanation for our results is that the presence of silacycloalkyl bridges increases the stabilities of the titanocene complexes. Furthermore, the molecular weight of the polyethylene ((1.3–2.6) × 10⁶ by GPC) obtained with **3** was larger than those produced by **4**. The molecular weight distributions (*M_w/M_n*) were approximately 2.0 for complex **3**, indicating that a single catalytic species was responsible for the polymerization.

In addition, the silacycloalkyl-bridged ansa-titanocene complexes (**3**) show higher activity than the acyclic dimethylsilyl analogue (**A**). In general, the larger dihedral angle (α) of a metallocene enlarges the reaction space between the two cyclopentadienyl ligands and increases the catalytic activity.^{13–15} Replacement of the dimethylsilyl bridge in **A** by the silacycloalkyl bridges in **3** results in an increase in the dihedral angle (α) (4–5°), leading to an increase in activity. The polymerization results suggest that bridge substituents have an important effect on activities through conformational effects. Given the similar electronic effects of the bridge silacycloalkyl group of **3** and acyclic **A**, it is reasonable to assume that conformational effects play a key role in the alteration of activities. It should be particularly noted that the CH₃ group in acyclic **A** can rotate freely around the Si–C bond. A possible reason cyclic ansa-titanocene complex **3** is more active than its acyclic counterpart **A** may be that the restricted rotation of the Si–C bond makes the silacycloalkyl group more conformationally stable and therefore more likely to accelerate the insertion of a monomer molecule.

The results additionally show that the activity of **3** increases with increasing size of the silacycloalkyl bridge and reaches a maximum in the six-membered

(12) (a) Brintzinger, H. H.; Fischer, D.; Mülhaupt, R.; Rieger, B.; Waymouth, R. M. *Angew. Chem., Int. Ed. Engl.* **1995**, *34*, 1143. (b) Mohring, P. C.; Coville, N. J. *J. Organomet. Chem.* **1994**, *479*, 1. (c) Kaminsky, W. *Catal. Today* **1994**, *20*, 257. (d) Halterman, R. L. *Chem. Rev.* **1992**, *92*, 965. (e) Jordan, R. F. *Adv. Organomet. Chem.* **1991**, *32*, 325.

(13) Piers, W. E.; Shapiro, P. J.; Bercaw, J. E. *Synlett* **1990**, *2*, 74. (14) Jeske, G.; Schock, L. E.; Swepston, P. N.; Schumann, H.; Marks, T. J. *J. Am. Chem. Soc.* **1985**, *107*, 8091.

(15) Obora, Y.; Tetsuo, O.; Stern, C. L.; Marks, T. J. *J. Am. Chem. Soc.* **1997**, *119*, 3745.

Table 7. Ethylene Polymerization of *ansa*-Metallocene Complexes^a

| entry | catalyst | n_{cat} (μmol) | time (min) | yield (g) | activity ^b | T_m ($^{\circ}\text{C}$) | M_w ($\times 10^6$) | M_w/M_n |
|-------|-----------------------|--------------------------------------|------------|-----------|-----------------------|------------------------------|-------------------------|-----------|
| 1 | 3a | 0.25 | 15 | 0.39 | 6.2 | 135.6 | 1.3 | 2.0 |
| 2 | 3b | 0.25 | 15 | 0.51 | 8.2 | 135.3 | 1.8 | 1.9 |
| 3 | 3c | 0.25 | 15 | 0.90 | 14 | 138.3 | 2.3 | 1.7 |
| 4 | 3d | 0.25 | 15 | 0.64 | 10 | 136.2 | 2.6 | 1.6 |
| 5 | standard ^c | 0.25 | 15 | 0.36 | 5.8 | 131.4 | 1.4 | 2.2 |
| 6 | 4a | 1 | 15 | 0.29 | 1.2 | 132.1 | 0.43 | 2.5 |
| 7 | 4b | 1 | 15 | 0.37 | 1.5 | 132.8 | 0.39 | 2.3 |
| 8 | 4c | 1 | 15 | 0.41 | 1.6 | 132.9 | 0.46 | 2.3 |
| 9 | 4d | 1 | 15 | 0.39 | 1.6 | 132.2 | 0.41 | 2.2 |
| 10 | standard ^d | 1 | 15 | 0.43 | 1.7 | 131.8 | 0.73 | 2.1 |

^a Polymerization conditions: ethylene pressure is 60 psig in 30 mL of *n*-hexane, Al:M = 1:5000 (M = Ti, Zr), 30 $^{\circ}\text{C}$. ^b 10^3 kg/mol_{cat} h. ^c Standard sample is Me₂SiCp₂TiCl₂ **A**. ^d Standard sample is Me₂SiCp₂ZrCl₂ **B**.

Table 8. Relative Energy Differences (in kcal/mol) among Three Species Existing in the Polymerization Path

| compound | $E_{\text{ethyl, propene}}$ | $E_{\text{propyl, ethene}}$ | E_{pentyl} |
|------------------------|-----------------------------|-----------------------------|---------------------|
| 3a | -3.9 | 0 | -22.4 |
| 3b | -4.2 | 0 | -23.0 |
| 3c (chair-form) | -3.7 | 0 | -23.2 |
| 3c (boat-form) | +0.7 | +4.4 | -2.8 |
| 3d | -3.9 | 0 | -22.2 |
| 4a | -4.5 | 0 | -15.2 |
| 4b | -4.9 | 0 | -16.0 |
| 4c (chair-form) | -1.8 | 0 | -13.0 |
| 4c (boat-form) | +2.7 | +4.3 | +3.2 |
| 4d | -4.7 | 0 | -15.6 |

silacyclohexyl-bridged *ansa*-titanocene complex **3c** (14×10^3 kg PE mol_{cat}⁻¹ h⁻¹). It is noteworthy that the silacycloalkane conformation gave rise to enhanced catalytic activity of the titanium center even though the cyclic ring and titanium center are remote from each other. To obtain information on the effect of the silacycloalkyl ring, density functional theory (DFT) calculations were performed, and the resulting energy profiles were examined.

In response to experimental findings, previous theoretical calculations have focused on the influence of the steric environment at the metal center.¹⁶ In this paper we use comparative X-ray crystallography and theoretical studies to analyze the steric changes that occur at the metal center in titanocene and zirconocene complexes as a result of silacycloalkyl ring substitution. To distinguish between the conformational effect of the ancillary cyclic rings on the structure and properties of *ansa*-metallocene complexes, we compare a series of compounds that have ligands with similar electron-donating abilities but different sizes, namely, silacyclobutyl- and silacyclopentyl-cyclopentadienyl versus silacyclohexyl-cyclopentadienyl. We investigate how the different ring bridges affect the catalytic behavior of (cyclo)SiCp₂MCl₂/MAO (M = Ti, Zr) in the ethylene polymerization reaction.

Calculations at the BP86 level of theory reveal that the energy minimum paths for the catalytic reaction steps primarily are confined to the singlet potential energy surface (PES). Table 8 summarizes the energetics of key stationary points along the reaction paths.

(16) Examples for recent work: (a) Yoshida, T.; Koga, N.; Morokuma, K. *Organometallics* **1995**, *14*, 746. (b) Meier, R. J.; van Doremale, G. H. J.; Iarlori, S.; Buda, F. *J. Am. Chem. Soc.* **1994**, *116*, 7274. (c) Weiss, H.; Ehrig, M.; Ahlrichs, R. *J. Am. Chem. Soc.* **1994**, *116*, 4919. (d) Guerra, G.; Cavallo, L.; Moscardi, G.; Vacatello, M.; Corradini, P. *J. Am. Chem. Soc.* **1994**, *116*, 2988. (e) Bierwagen, E. P.; Bercaw, J. E.; Goddard, W. A., III. *J. Am. Chem. Soc.* **1994**, *116*, 1481. (f) Gleiter, R.; Hyla-Krispin, I.; Niu, S.; Erker, G. *Organometallics* **1993**, *12*, 3828.

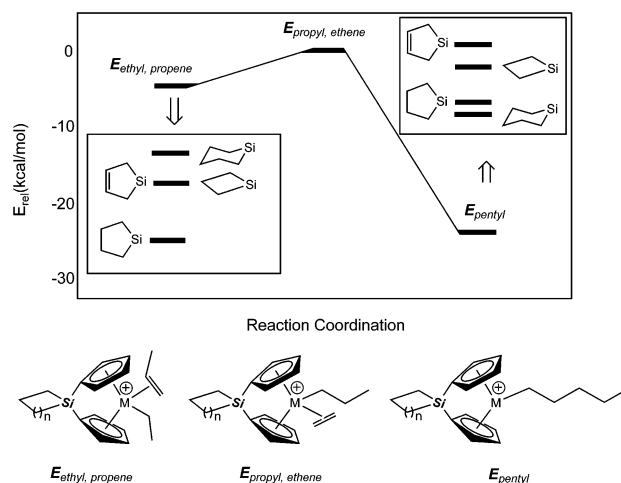
**Figure 5.** Energy profiles of *ansa*-metallocenes.

Figure 5 plots the energy profile for the most feasible chain propagation and termination reaction steps. The conformations of the involved species along the reaction paths are also depicted in Figure 5. All optimized structures are provided as Supporting Information. As for the model system, the “real” cationic metal(IV) alkyl complex is a metal-propylene complex (Figure 5, center) that is higher in energy than a metal-ethylpropene complex (Figure 5, left) and higher than a metal-pentyl complex (Figure 5, right). An increase in the ring size accelerates the formation of the insertion precursor pentyl complex, whereas termination becomes less favorable, since the energy level of the ethylpropene complex is increased. Therefore, more favorable formation of a pentyl complex and less favorable formation of an ethylpropene complex should give a catalyst better activity.

As can be seen in Table 8, a titanium complex might be a better catalyst than a zirconium complex because of the larger energy difference between the metal-propylene complex and metal-pentyl complex. Among titanium complexes, the chair form of the silacyclohexyl bridge should be the best catalyst. By introducing a silacyclohexyl bridge, the termination energy for the ethylpropene complex is reduced (-3.7 kcal mol⁻¹) and the pentyl complex (propagation precursor) can be stabilized (-23.2 kcal mol⁻¹).

Summary

The silacycloalkyl bridge of the ligand forms a wide gap in the equatorial plane of the complexes that may allow selective access of substrate molecules to the

Lewis acidic metal centers. Therefore, we prepared and structurally characterized a series of silacycloalkyl-bridged *ansa*-metallocene complexes (**3**–**5**), demonstrating the utility of 1,1-dicyclopentadienyl-1-silacycloalkane or -alkene systems as potential catalysts for the polymerization of ethylene. While conformationally less stable silacyclobutyl- and pentyl-bridged complexes (**3a** and **3b**) exhibit good ethylene polymerization activity ($(6\text{--}8) \times 10^3$ kg PE mol_{cat}⁻¹ h⁻¹) in the presence of methylalumoxane, the conformationally stable chair form of silacyclohexyl complex (**3c**) shows much higher activity (14×10^3 kg PE mol_{cat}⁻¹ h⁻¹) for ethylene polymerization when it is activated with MAO. In particular, *ansa*-titanocene complex catalysts show much higher activities than the *ansa*-zirconocene complex variants and produce very high molecular weight polyethylenes ($(1.3\text{--}2.6) \times 10^6$ by GPC).

Experimental Section

General Procedures. All manipulations were performed under a dry, oxygen-free nitrogen or argon atmosphere using standard Schlenk techniques or in a Vacuum Atmospheres HE-493 drybox. Diethyl ether, toluene, hexane, and pentane were distilled under nitrogen from sodium/benzophenone. Dichloromethane was dried with CaH₂. Benzene-*d*₆ was distilled under nitrogen from sodium and stored in a Schlenk storage flask until needed. CDCl₃ was predried under CaH₂ and vacuum-transferred. *n*-BuLi (1.6 M in hexanes), MeMgBr, and MCl₄ (M = Ti, Zr, Hf) were used as received from Aldrich. 1,1-Dichloro-1-silacyclobutane, 1,1-dichloro-1-silacyclopentane, 1,1-dichloro-1-silacyclohexane, and 1,1-dichloro-1-silacyclopent-3-ene were prepared as described in the literature.⁵ All ¹H (300.1 MHz, measured in CDCl₃) and ¹³C (75.4 MHz, measured in CDCl₃) NMR spectra were recorded on a Varian Mercury-300BB spectrometer except where indicated otherwise. ¹H and ¹³C NMR chemical shifts are reported relative to Me₄Si and were determined by reference to the residual ¹H or ¹³C solvent peaks. Elemental analyses were performed with a Carlo Erba Instruments CHNS-O EA1108 analyzer.

Preparation of 1,1-Dicyclopentadienyl-1-silacycloalkane or -alkene (2). Representative procedure: cyclopentadiene (4.0 g, 60.5 mmol) in THF (100 mL) was added to a 250 mL flask equipped with a magnetic stirrer, an argon inlet, and a condenser. The solution was cooled to 0 °C, and then *n*-BuLi (37.9 mL, 1.6 M in hexanes) was added dropwise. The reaction mixture was warmed to room temperature and stirred for an additional 12 h. The resulting solution was cooled to 0 °C, and then (cyclo)SiCl₂ (27.51 mmol) was added. The mixture was heated at reflux for 2 h. The mixture was then stirred for 12 h at room temperature, after which all volatiles were removed by drying in vacuo. The resulting residue was extracted with pentane, filtered through a Celite pad, and dried in vacuo to afford a pale yellow oil.

2a: colorless oil (3.14 g, 57%) obtained by vacuum distillation (37 °C, 0.3 Torr). Elemental analysis for C₁₃H₁₆Si: found C 77.85, H 8.12; calcd C 77.93, H 8.05.

2b: colorless oil (3.20 g, 54%) obtained by vacuum distillation (55 °C, 0.3 Torr). Elemental analysis for C₁₄H₁₈Si: found C 78.75, H 8.50; calcd C 78.44, H 8.46.

2c: colorless oil (4.01 g, 64%) obtained by vacuum distillation (68 °C, 0.3 Torr). Elemental analysis for C₁₅H₂₀Si: found C 78.91, H 8.85; calcd C 78.88, H 8.83.

2d: colorless oil (2.59 g, 44%) was obtained by vacuum distillation (75 °C, 0.3 Torr). Elemental analysis for C₁₄H₁₆Si: found C 79.22, H 7.61; calcd C 79.18, H 7.59.

Preparation of the *ansa*-Metallocene Complexes, (cyclo)SiCp₂MCl₂ (M = Ti, **3; Zr, **4**; Hf, **5**).** Representative procedure: *n*-BuLi (1.3 mL, 1.6 M in hexanes) was added to a

solution of **2** (1.0 mmol) in diethyl ether (20 mL) that was precooled to -78 °C. The reaction mixture was warmed to room temperature and stirred for 2 h, after which it was transferred via cannula to a suspension of titanium tetrachloride (1.1 equiv) in Et₂O (20 mL) that was cooled to -78 °C. The resultant yellow mixture was allowed to warm to room temperature and stirred for 2 h. Removal of the volatiles provided the final crude product, which was further crystallized from pentane at -45 °C to provide pure (cyclo)Si(NBu)₂-TiCl₂ (**3**) as a red-yellow solid.

3a: red crystals (0.12 g, 38%) obtained by recrystallization (-45 °C, pentane). Elemental analysis for C₁₃H₁₄Cl₂SiTi: found C 48.86, H 4.18; calcd C 49.24, H 4.45.

3b: red crystals (0.15 g, 45%) obtained by recrystallization (-45 °C, pentane). Elemental analysis for C₁₄H₁₆Cl₂SiTi: found C 50.39, H 4.58; calcd C 50.78, H 4.87.

3c: red crystals (0.23 g, 67%) obtained by recrystallization (-45 °C, pentane). Elemental analysis for C₁₅H₁₈Cl₂SiTi: found C 51.79, H 4.95; calcd C 52.19, H 5.26.

3d: red crystals (0.19 g, 58%) obtained by recrystallization (-45 °C, pentane). Elemental analysis for C₁₄H₁₄Cl₂SiTi: found C 50.79, H 4.09; calcd C 51.09, H 4.29.

4a: yellow crystals (0.17 g, 47%) obtained by recrystallization (-45 °C, pentane). Elemental analysis for C₁₃H₁₄Cl₂SiZr: found C 43.60, H 4.02; calcd C 43.32, H 3.91.

4b: yellow crystals (0.15 g, 40%) obtained by recrystallization (-45 °C, pentane). Elemental analysis for C₁₄H₁₆Cl₂SiZr: found C 44.61, H 4.20; calcd C 44.90, H 4.31.

4c: yellow crystals (0.19 g, 49%) obtained by recrystallization (-45 °C, pentane). Elemental analysis for C₁₅H₁₈Cl₂SiZr: found C 46.07, H 4.54; calcd C 46.37, H 4.67.

4d: yellow crystals (0.17 g, 46%) obtained by recrystallization (-45 °C, pentane). Elemental analysis for C₁₄H₁₄Cl₂SiZr: found C 44.90, H 3.69; calcd C 45.14, H 3.79.

5a: yellow crystals (0.29 g, 65%) obtained by recrystallization (-45 °C, pentane). Elemental analysis for C₁₃H₁₄Cl₂SiHf: found C 34.74, H 3.14; calcd C 34.87, H 3.15.

5b: yellow crystals (0.33 g, 71%) obtained by recrystallization (-45 °C, pentane). Elemental analysis for C₁₄H₁₆Cl₂SiHf: found C 36.29, H 3.48; calcd C 36.42, H 3.49.

5c: yellow crystals (0.34 g, 71%) obtained by recrystallization (-45 °C, pentane). Elemental analysis for C₁₅H₁₈Cl₂SiHf: found C 37.73, H 3.79; calcd C 37.87, H 3.81.

5d: yellow crystals (0.30 g, 65%) obtained by recrystallization (-45 °C, pentane). Elemental analysis for C₁₄H₁₄Cl₂SiHf: found C 36.44, H 3.06; calcd C 36.58, H 3.07.

Preparation of Dimethyl Derivatives of *ansa*-Titanocene Complexes, (cyclo)SiCp₂TiMe₂ (6**).** Representative procedure: MeMgBr (3.0 M in ether, 0.80 mL, 2.4 mmol) was added to a solution of **3** (1.0 mmol) in diethyl ether (20 mL) that was precooled to -78 °C. The reaction mixture was warmed to room temperature and stirred for 2 h. The resulting yellow solution was dried under vacuum to afford a pale yellow solid. The solid was extracted with pentane, and the filtrate was concentrated and cooled to -45 °C. Yellow solid **6** was isolated by filtration, washed with cold pentane, and dried in vacuo.

6a: yellow powder (0.20 g, 72%) obtained by recrystallization (-45 °C, pentane). Elemental analysis for C₁₅H₂₀SiTi: found C 64.85, H 7.11; calcd C 65.21, H 7.30.

6b: yellow powder (0.19 g, 65%) obtained by recrystallization (-45 °C, pentane). Elemental analysis for C₁₆H₂₂SiTi: found C 65.84, H 7.44; calcd C 66.20, H 7.64.

6c: yellow powder (0.23 g, 76%) obtained by recrystallization (-45 °C, pentane). Elemental analysis for C₁₇H₂₄SiTi: found C 66.63, H 7.75; calcd C 67.09, H 7.95.

6d: yellow powder (0.25 g, 87%) obtained by recrystallization (-45 °C, pentane). Elemental analysis for C₁₆H₂₀SiTi: found C 66.30, H 6.71; calcd C 66.66, H 6.99.

Polymerization of Ethylene. Hexane (30 mL) was added to a dried 70 mL glass reactor in a glovebox. The reactor was

assembled and brought out of the glovebox. The reactor was immersed in an oil bath whose temperature had been set to 30 °C, and the solvent was stirred for 15 min. An activated catalyst prepared by mixing 0.25 μmol of catalyst and MAO (0.34 g, 0.8 mmol of Al) was added via syringe. Ethylene was fed immediately under the predetermined pressure (60 psig). After a given time (15 min), the polymerization reaction was quenched by venting ethylene and pouring the mixture into acetone. A white precipitate was collected by filtration and dried under vacuum. Table 7 summarizes the polymerization results; $\text{Me}_2\text{SiCp}_2\text{MCl}_2$ (M = Ti, **A**; Zr, **B**) was used for comparison.

Crystal Structure Determination. Crystals of **3b**, **3c**, **4b**, and **4c** were obtained from toluene, sealed in glass capillaries under argon, and mounted on the diffractometer. Data were collected and corrected for Lorentz and polarization effects. Each structure was solved by the application of direct methods using the SHELXS-96 program,^{17a} and least-squares refinement was performed using SHELXL-97.^{17b} After anisotropic refinement of all non-H atoms, several H atom positions could be located in difference Fourier maps. These were refined isotropically, while the remaining H atoms were calculated in idealized positions and included into the refinement with fixed atomic contributions. Further detailed information is listed in Table 1.

Computational Details. Stationary points on the potential energy surface were calculated using the Amsterdam Density Functional (ADF) program, developed by Baerends et al.^{18,19} and vectorized by Ravenek.²⁰ The numerical integration scheme applied for the calculations was developed by te Velde et al.^{21,22} The geometry optimization procedure was based on the method of Versluis and Ziegler.²³ The electronic configurations of the molecular systems were described by double- ζ STO basis sets with polarization functions for the H and C atoms, and triple- ζ Slater-type basis sets were employed for the Si,

Ti, and Zr atoms.^{24,25} The 1s electrons of C, the 1s–2p electrons of Si and Ti, and the 1s–3d electrons of Zr were treated as frozen cores. A set of auxiliary²⁶ s, p, d, f, and g STO functions, centered on all nuclei, was used to fit the molecular density and the Coulomb and exchange potentials in each SCF cycle. Energy differences were calculated by augmenting the local exchange–correlation potential²⁷ with Becke's²⁸ nonlocal exchange corrections and Perdew's²⁹ nonlocal correlation corrections (BP86). Geometries were optimized including nonlocal corrections at this level of theory. First-order Pauli scalar relativistic corrections^{30,31} were added variationally to the total energy for all systems. In view of the fact that all systems investigated in this work show a large HOMO–LUMO gap, a spin-restricted formalism was used for all calculations. No symmetry constraints were used.

Acknowledgment. This work was supported by the Korea Research Foundation Grant (KRF-2002-013-E00071) and Grant No. R02-2002-000-00147-0 from the Basic Research Program of the Korea Science and Engineering Foundation.

Supporting Information Available: Crystallographic data (excluding structure factors) for the structures **2a**, **2b**, **3a**, **4b**, and **4c** reported in this paper and listings giving optimized geometries of the crucial structures are included (Cartesian coordinates, in Å). This material is available free of charge via the Internet at <http://pubs.acs.org>.

OM030287J

(24) Snijders, J. G.; Baerends, E. J.; Vernoijs, P. *At. Nucl. Data Tables* **1982**, *26*, 483.

(25) Vernoijs, P.; Snijders, J. G.; Baerends, E. J. *Slater Type Basis Functions for the Whole Periodic System*; Internal Report (in Dutch); Department of Theoretical Chemistry, Free University: Amsterdam, The Netherlands, 1981.

(26) Krijn, J.; Baerends, E. J. *Fit Functions in the HFS Method*; Internal Report (in Dutch); Department of Theoretical Chemistry, Free University: Amsterdam, The Netherlands, 1984.

(27) Vosko, S. H.; Wilk, L.; Nusair, M. *Can. J. Phys.* **1980**, *58*, 1200.

(28) Becke, A. *Phys. Rev. A* **1988**, *38*, 3098.

(29) (a) Perdew, J. P. *Phys. Rev. B* **1986**, *34*, 7406. (b) Perdew, J. P. *Phys. Rev. B* **1986**, *33*, 8822.

(30) Snijders, J. G.; Baerends, E. J. *Mol. Phys.* **1978**, *36*, 1789.

(31) Snijders, J. G.; Baerends, E. J.; Ros, P. *Mol. Phys.* **1979**, *38*, 1909.

(17) (a) Sheldrick, G. M. *Acta Crystallogr., Sect. A* **1990**, *A46*, 467. (b) Sheldrick, G. M. *SHELXL*, Program for Crystal Structure Refinement; University of Göttingen: Germany, 1997.

(18) Baerends, E. J.; Ellis, D. E.; Ros, P. *Chem. Phys.* **1973**, *2*, 41.

(19) Baerends, E. J.; Ros, P. *Chem. Phys.* **1973**, *2*, 52.

(20) Ravenek, W. In *Algorithms and Applications on Vector and Parallel Computers*; te Riele, H. J. J., Dekker, T. J., van de Horst, H. A., Eds.; Elsevier: Amsterdam, The Netherlands, 1987.

(21) te Velde, G.; Baerends, E. J. *J. Comput. Chem.* **1992**, *99*, 84.

(22) Boerrigter, P. M.; Velde, G. T.; Baerends, E. J. *Int. J. Quantum Chem.* **1988**, *33*, 87.

(23) Versluis, L.; Ziegler, T. *J. Chem. Phys.* **1988**, *88*, 322.